

# METHOD OF LIFETIME PREDICTION FOR SAILPLANE FIBRE STRUCTURES

By Christoph W. Kenschke

Presented at the XXV OSTIV Congress 1997, Saint Auban sur Durance, France.

## SUMMARY

A method of lifetime prediction for sailplane structures made from glass fibre reinforced plastics (GFRP) is presented. The procedure is based on the application of the linear Palmgren-Miner rule, constant amplitude life diagrams which are derived from s-n curves for glass epoxy (GI-Ep) and unsaturated glass polyester (GI-UP) respectively, and the wind energy-specific WISPER-load sequence. The resulting prediction is compared with load spectra tests on the same specimens as used for the s-n curves. The accuracy is satisfactory. However, the conformity of the test results and the prediction also depends on the scatter of the tests and the applied survivability (here 95%). The applications of safety factors and the influence of stress concentrations in load introduction parts of wing structures are discussed.

## 1. INTRODUCTION

Since sailplanes are of a composite materials design, their service life certification suffers from the suspicious eyes of the authorities because the fatigue behavior of e.g. GFRP was not known or understood well enough. Knowing more about fatigue problems on metals, the allowables for the admitted lifetime of composite materials were handled rather conservatively. In small steps, the service life was increased from 3000 over 6000 to the present 12000 flight hours. Extensive and expensive structural tests on wings and components were necessary to get this status. It is foreseeable — and perhaps it has already happened — that at some sites with excellent weather and/or training conditions, sailplanes have again reached the certified lifetime limit.

Thanks to an Australian initiative, a Janus wing was

fatigue-tested at the RMIT with a higher load level than designed for, simulating a similar lifetime with a service life specifically adopted to the Australian conditions. As an important result it is reported that the load bearing composite parts, like the glass fibre strengthened spars, endured in principle the very hard service life program without severe damages, while fittings and other parts easily to be inspected had to be repaired or replaced (1). The test also demonstrated that only a service life test at elevated strain level shows a result in a reasonable time, whereas a test applying just the limit design load to a real structure would have run forever. It can also be stated that the fatigue behavior of GFRP is superior to metal structures.

Therefore it is proposed to include the knowledge about the very good fatigue properties of composites into the certification considerations of composite gliders. For example, the fatigue properties of GI-Ep and GI-UP are extensively investigated in the meantime on small scale specimens. For example under the application in rotor blades of wind turbines there exists a sufficient amount of data sets from which information can also be used for lifetime calculations of GFRP sailplanes (2,3,4).

In this paper, a lifetime prediction method is presented which uses such data in combination with the linear Palmgren-Miner rule and an established service life program. The s-n curves and the derived constant-amplitude-life diagrams for the presented example are reported in (3) and (4). A survey of the investigated materials is given in Table 1. The tests with GI-Ep were carried out at DLR/D, with GI-UP1 at ECN/NL and with GI-UP2 (manufactured by Riso/DK) at NLR/NL.

## 2. LIFETIME PREDICTION

### 2.1 S-n curves and scatter

The basis for a good lifetime prediction are the s-n or Wöhler-curves of the materials the concerned structure is made from. By convention, they are presented in stress ( $\sigma$ ) or strain ( $\epsilon$ ) versus number of cycles n either in a lin-log plot for constant stress ratios R which are defined as

where  $\sigma_u$  is the lowest stress and  $\sigma_o$  the highest stress,

$$R = \frac{\sigma_u}{\sigma_o}$$

Laminate	Combination	Manufacturing method
Glass-Epoxy (GI-Ep)	$\pm 45^\circ / UD, UD$	Hand laminate (Industry)
Glass-Polyester (GI-UP1)	$0^\circ / Random$	Hand laminate (Industry)
Glass-Polyester (GI-UP2)	$\pm 45^\circ / 0^\circ$	Winding (laboratory)

Table 1: Reference materials.

tension is positive, compression negative.

For fibre composites, the  $\epsilon$ -n (strain versus load cycles) presentation is recommended, since optimally the main fibre direction is orientated in the designated load direction. The failure strain of the whole compound is dominated by the fibres. Thus, via strain presentation, an objective comparison of fatigue curves of different composites is possible. The failure stresses depend strongly on the different fibre orientations of a composite lay up, as well as on the fibre content. In this case, for a comparison the E-modulus must be included. Specific testing methods often depend on the combination of the investigated laminates. Good experience is available and described in (3) and (5).

There are various methods for the statistical evaluation of the fatigue data. The linear regression in a log-log scale is very simple and achieves good results especially in the high-cycle range. This advantage is used by a method proposed by Sendeckyj (6), which additionally considers the static test data and the behavior in the low-cycle range. His method is based on a 2-parametric Weibull distribution including Halpin's "wearout" model (7). It is widely used in aerospace design and also chosen for our application. The curve is described according to the equation:

$$\epsilon_a = \beta \cdot \frac{(-\ln P(N))^{\frac{1}{\alpha}}}{((N-A) \cdot C)^S} \cdot e^{-\frac{U_\gamma(P(N))}{\sqrt{n} \cdot \alpha}}$$

It considers survivability and confidence limits.  $\epsilon_a$  is the maximum strain applied,  $\beta$  the scale, and  $\alpha$  the shape parameter of the Weibull distribution. N is the number of cycles to failure and P(N) the probability of survival. A stands for  $-(1-C)/C$ . S defines the slope in the high cycle range. In the presentation of the slope, often its reciprocal value k is used. Certification rules for wind turbine fatigue design e.g. use  $k=10$  for GI-Ep and  $k=9$  for GI-UP at a stress ratio of  $R=-1$  (8). The other parameter, C, allows for flattening or steepening the slope of the curve at low cycles.

The second part of the equation considers the confidence bounds. Here,  $U_\gamma(P(N))$  is the percentage point of the survivability. According to the above mentioned certification rules (8), a survivability  $P(N) = 95\%$  with a lower confidence limit of  $\gamma = 95\%$  is taken into account. Figure 1 shows the curves for the percentage  $U_\gamma(P(N))$  for fatigue test data

	Shape parameter $\alpha$	Scale parameter $\beta$	Slope S	$k=1/S$	C
R=10 ( $\pm 45^\circ$ /UD lay up)	17.429	2.190	0.092	10.87	0.00018
R=-1 ( $\pm 45^\circ$ /UD lay up)	13,9878	2.23027	0.0868	11.52	0.22
R=0.1 (UD lay up)	16.482	2.25	0.1105	9.05	0.00146

Table 2: Fatigue evaluation parameters for GI-Ep with  $\pm 45^\circ$ /UD lay up (R = -1, 10) and UD lay up (R = 0.1)

from  $10 < n < 80$  (excerpt from Bain (9)).

A big advantage of the method is also the possibility to consider residual strengths, runouts, and doubtful test

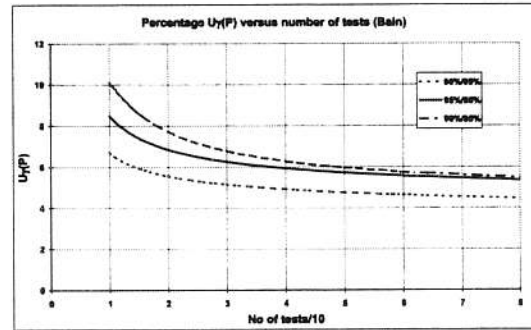


Figure 1: Percentage curves  $U_\gamma(P(N))$  for 3 different survivabilities with 95% lower confidence limit (9).

data. As an example for the proposed fatigue evaluation, Figure 2 shows an  $\epsilon$ -n curve for GI-Ep with a  $\pm 45$  degree/UD lay up corresponding to Table 1 which results from investigations described in (3), (4) and (5). The upper curve represents the mean curve, the lower one the 95% survivability with the 95% lower confidence limit.

The parameters for the fatigue curves of the GI-Ep materials used for the stress ratios  $R=0.1$  (tension-tension), -1

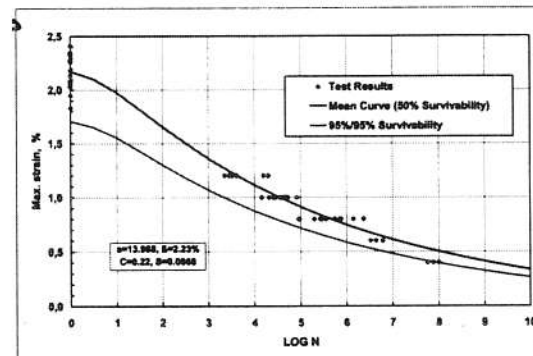


Figure 2: Fatigue evaluation of  $45^\circ$ /UD GI-Ep from data with 57 tests at  $R = .1$ .

(tension-compression) and 10 (compression-compression) are shown in Table 2.

The shape parameter  $\alpha$  is a measure for the scatter in the data set. The larger the shape parameter  $\alpha$ , the lower the scatter. For high performance composites in aerospace using prepreg technology (pre-impregnated fibre weaves) a mean value of 20 is well experienced (10). The data presented in this report result mainly from hand lay up manufactured specimens, thus yielding larger scatter.

The application of a certain survivability on fatigue curves which may have different mean values can compensate such discrepancies. E.g. in Figure 3 a significant difference is shown in the mean fatigue curves of different GI-UP materials and specimens tested at two institutes, due to different scatter. However, the curves of 95% survivability are nearly identical. This influences also the lifetime prediction as described later.

## 2.2 Constant amplitude life (Haigh-) diagram

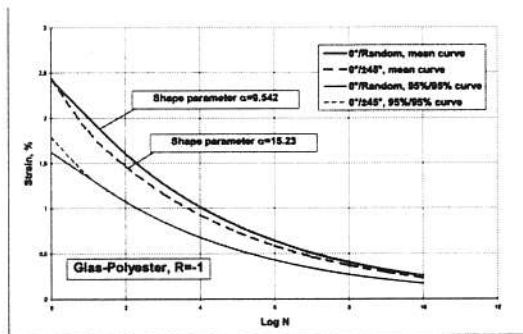


Figure 3: Influence of the scatter on the lifetime prediction.

The damage propagation in a composite structure not only depends on the amplitudes and load cycles which stochastically occur during the service life, but also from the mean value of the stress and the stress ratio  $R$ . For a fair judgment about their influence on the lifetime, a constant amplitude life (Haigh-) diagram can give information. A common procedure is the construction of this diagram from three fatigue curves achieved at stress ratios of  $R = 0.1, -1$  and  $10$ . This will normally result in sufficiently reliable data. Testing of more stress ratios would lead to unnecessary high costs. Figure 4 contains the fatigue curves for GI-Ep described in Table 2. They are presented with the 95% survivability and 95% lower confidence limit. For  $R = 0.1$  no  $\pm 45^\circ$ /UD data are available, thus data from a pure UD-laminate were used, since for  $R = .1$  the two laminates have very low differences (3).

The Haigh-diagram is designed for lines of constant lifetimes which are derived from the  $\epsilon$ - $n$  curves by the consideration of the amplitudes versus mean values of stresses or

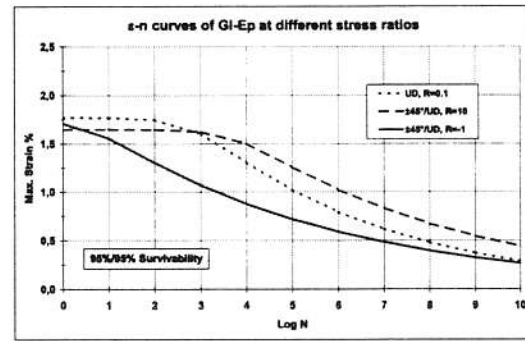


Figure 4:  $\epsilon$ - $n$  curves for GI-Ep at stress ratios of  $R = 0.1, -1$  and  $10$  (95% survivability, 95% lower confidence limit).

in our case, strains. For the mean curves (50% survivability) described above, the static values, which are identical with the scale parameters of the relevant curves are plotted in Figure 5.

By means of the Haigh-diagram it is now easy to get information about the damage accumulation which occurs due to other stress ratios and mean values than shown by

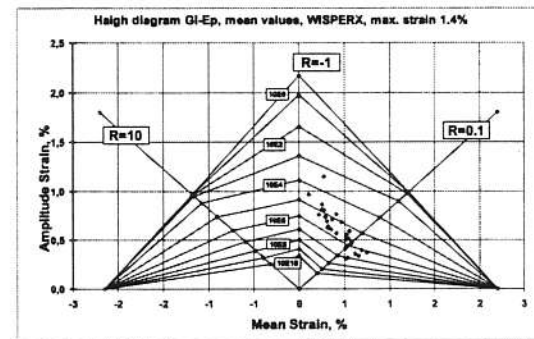


Figure 5: Constant amplitude life diagram (Haigh-diagram) for GI-Ep (50% survivability).

the measured curves. This is done by logarithmic interpolation between points of constant lifetime on the radials and linear interpolation between different radials and the static values. Instead of the linear interpolation, splines of higher order could also be used, however, this would lead to higher numerical effort. Beyond that the results of the various spline methods are not thought to differ significantly. A comparison between a polygon and a cubic spline interpolation showed only 15% difference in lifetime (3).

### 2.3 Load sequence

For the lifetime prediction the wind energy load sequence (standard) WISPER was used as well as its reduced version WISPERX (11). The sailplane standard KoSMOS could not yet be referred to as at the time of writing this report, neither experimental life cycle data for GFRP with KoSMOS nor a suitable lifetime prediction algorithm were available. However, for explaining the calculation method WISPER is well qualified, since it is well described and experimental data are available, too.

The WISPER/WISPERX standards which were analyzed by the rainflow counting algorithm which are used for the purpose of comparing, for example, material properties and methods of lifetime prediction. The WISPER sequence is a row of integers ranging from 1 to 64 with zero level at 25 and maximum load at level 64. In practice the levels of a rainflow counted load sequence is multiplied by a certain factor in order to obtain the desired maximum load or strain level. WISPERX resulted from omitting amplitudes lower than 25% of WISPER, i.e. ranges lower than level 17. By definition, one life cycle (which contains 132,711 load cycles for WISPER and 12,831 load cycles for WISPERX) is representative for a 2 month operation time of a fictive wind turbine. Although this is not comparable with a real wind turbine, the life cycle presentation of the WISPER standards may give a good impression of a possible lifetime.

Transitions of the sequence with a standard deviation lower than 6.5% in relation to their mean stress value were pooled (11). Mean value and amplitude can be defined in relation to a certain strain value. As an example, these values are plotted as dots in Figure 5 for a hypothetical design strain of 1.4%. For each of the points in Figure 5 the possible number of load cycles has to be found by interpolation between the radials and the lines of constant lifetime and then be compared with the load cycle number of a WISPER or WISPERX life cycle. As an example, Table 3 contains these data for a design strain level of 1.4% together with the corresponding ranges, standard deviation and load cycle numbers of WISPERX.

### 2.4 Linear Palmgren-Miner rule

$$D = \sum_{i=1}^k \frac{n_i}{N_i} = 1,$$

A widely used method for damage accumulation is the linear Palmgren-Miner rule, which is

where  $k$  is the sum of the load steps,  $n_i$  the number of sequence load cycles at strain  $\epsilon_i$  and  $N_i$  the number of load cycles to failure at  $\epsilon_i$ .  $D$  depends mainly on the load spectrum, the working stress level and the composite lay-up.

Although this method originally was applied to metals, and there also is no obvious physical justification for its application on composites, it is, because of its simplicity, highly attractive. Experience has shown that the value of  $D$  can vary over a wide range, from  $10^{-1}$  to  $0^1$ , for metals as well as for composites. If the experimentally obtained number of cycles or passes through the sequence, are higher than the calculated one, the lifetime estimation is conservative. The validation of the Palmgren-Miner rule by means of wind-energy specific standards is anticipating to justify the application of the same rule for sailplanes also.

### 2.5 Load sequence measurements on GFRP

WISPER sequence tests were carried out at ECN/NL with GI-UP1, WISPERX tests at DLR with GI-Ep. The data were statistically evaluated corresponding to the  $\epsilon$ - $n$  curves as mean curves and curves of 95% survivability and 95% lower confidence limit. The scale of lifetime is plotted in cycles of WISPER/WISPERX.

## 3. COMPARISON OF MEASUREMENT AND PREDICTION

### 3.1 WISPERX, GI-Ep

Lifetime calculations were carried out for both mean values (Figure 6) and values of 95% probability/95% lower confidence limit (Figure 7) to get an impression about the influence of the scatter. In Figure 6 the mean prediction curve is slightly underneath the mean curve of the test data, i.e. it is conservative but very close to the measurements. The 95%/95% curves in Figure 7 fit very well as a maximum spectrum strain of 1%, the prediction curve is, however, slightly divergent towards the lower maximum strains, i.e. conservative in the realistic application area of the design strains of rotor blades or glider wings with GFRP spar caps. The better congruence of the 95%/95% curves indicates that the shape parameter  $\alpha$  of the measured spectra data is lower than the prediction curve based on the constant amplitude  $\epsilon$ - $n$  data. This corresponds to a higher scatter of the spectra data or a lower number of data points respectively which indeed is the fact.

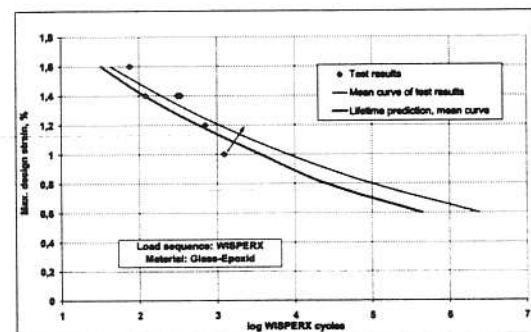


Figure 6: Comparison of lifetime prediction and GI-Ep data for mean values with WISPERX.

Range-Size (Levels)	Load cycle number	Stress ratio R	mean strain %	amplitude	Possible load cycle number	Damage accumulation
63	1	-0,62	0,269	1,148	2,85E+03	0,000350877
54	1	-0,80	0,108	0,969	3,00E+04	3,33333E-05
48	4	-0,55	0,251	0,866	4,40E+04	9,09091E-05
46	6	-0,53	0,251	0,818	7,20E+04	8,33333E-05
45	4	-0,50	0,269	0,808	7,80E+04	5,12821E-05
43	3	-0,30	0,413	0,767	6,00E+04	0,00005
42	2	-0,56	0,215	0,764	2,00E+05	0,00001
41	4	-0,44	0,287	0,739	1,70E+05	2,35294E-05
40	2	-0,33	0,359	0,713	1,30E+05	1,53846E-05
39	4	-0,39	0,305	0,695	2,40E+05	1,66667E-05
38	2	-0,19	0,467	0,686	1,00E+05	0,00002
36	6	-0,33	0,323	0,641	4,05E+05	1,48148E-05
35	9	-0,34	0,309	0,627	5,10E+05	1,76471E-05
34	10	-0,27	0,352	0,612	5,00E+05	0,00002
33	2	-0,03	0,556	0,591	1,80E+05	1,11111E-05
32	8	-0,16	0,413	0,570	5,10E+05	1,56863E-05
31	19	-0,03	0,524	0,557	3,00E+05	6,33333E-05
30	7	-0,02	0,517	0,538	4,05E+05	1,7284E-05
29	60	0,03	0,549	0,517	4,16E+05	0,000144231
28	36	0,01	0,517	0,507	6,00E+05	0,00006
27	26	0,09	0,582	0,486	5,00E+05	0,000052
26	144	0,11	0,582	0,466	6,00E+05	0,00024
25	30	0,10	0,546	0,446	1,00E+06	0,00003
24	586	0,09	0,513	0,429	1,75E+06	0,000334857
23	560	0,11	0,510	0,409	2,20E+06	0,000254545
22	1264	0,27	0,693	0,398	1,00E+06	0,001264
21	2666	0,33	0,747	0,376	1,05E+06	0,002539048
20	2450	0,26	0,617	0,363	3,30E+06	0,000742424
19	3218	0,32	0,657	0,338	4,40E+06	0,000731364
18	8614	0,25	0,535	0,321	1,00E+07	0,0008614
17	5914	0,25	0,513	0,308	1,80E+07	0,000328556
<b>Damage accumulation sum:</b>						<b>8,49E-03</b>
<b>Possible No of life cycles of WISPERX:</b>						<b>117,82</b>

Table 3: Example for lifetime calculation of UD GI-Ep with WISPERX for 50% survivability and design strain of 1.4%.

### 3.2 WISPER, GI-UP1 AND GI-UP2

For the lifetime calculation with glass-polyester, 2 Haigh-diagrams were designed. They differ in the data sets at R=0.1. The reason was that data of ECN at this stress ratio were available for the same material (GI-UP1) as for R=1. On the other hand, for R=0.1 also a data set from Risø/NLR (GI-UP2) was used, since the  $\epsilon$ -n curve yields lower values in the high cycle area, exceeds however the GI-UP1 curve in the low cycle range (12). Also for this comparison, mean values (Figure 8) and 95%/95% curves (Figure 9) were

evaluated. Figure 8 shows an optimistic prediction for GI-UP1 for the mean value presentation. In Figure 9, however, the 95%/95% prediction curves are very close together, again demonstrating the influence of the scatter. The congruence with the curve of the measured data is very good, especially in the range below about 1.1%.

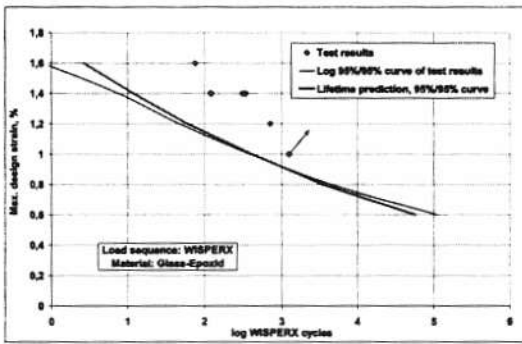


Figure 7: Comparison of lifetime prediction and GI-Ep data for 95% 95% values with WISPERX.

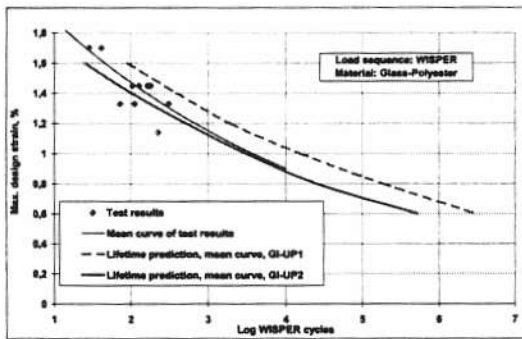


Figure 8: Comparison of lifetime prediction and GI-UP data for mean values with WISPER.

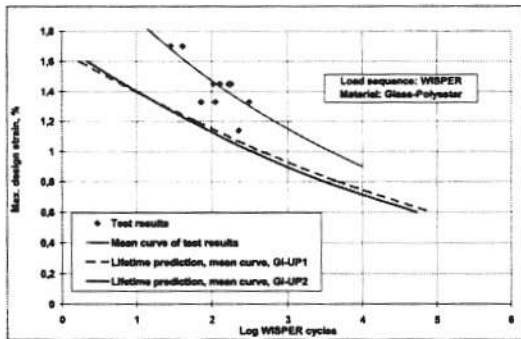


Figure 9: Comparison of lifetime prediction and GI-UP data for 95% 95% values with WISPER.

#### 4. DISCUSSION

The proof of any lifetime prediction method suffers from the fact that the experimental fatigue data can be achieved only in the high amplitude range (e.g. GFRP strains of 0.8% to 1.6%), whereas at the lower amplitudes where we commonly have the relative low design stresses (e.g. 0.3% to 0.7%), the testing time would be too long. Thus, an extrapolation of the load sequence and the prediction curves towards lower design levels than approved is necessary for the lifetime prediction. This inhibits, however, a certain lack of accuracy. So, for GI-Ep at decreasing load levels the prediction is more conservative in comparison to the extrapolation of the experimentally established curve, whereas in the same case, GI-UP tends slightly towards the experimental curve.

Therefore, the discussion of the performed lifetime evaluation is limited here to a design strain level of 1% because at that level measurements are still available. In Table 4 the damage accumulation sums are presented, which are derived from the curves of lifetime prediction and the curves evaluated from the load sequence tests on GI-Ep, GI-UP1 and GI-UP2. It is shown that the damage sum for GI-Ep with 2.27 is conservative whereas it is a bit optimistic but very close to 1 for the 95%/95% case. For GI-UP2, it is conservative but close to the experimental data.

The results of the lifetime prediction for both GI-Ep and GI-UP are not quite satisfactory, since at the moment they cannot be explained physically. Nevertheless they are in the tolerance bounds which are commonly found for metals. In the case for example, GI-UP1, the relative Miner rule would be used for the purpose of further lifetime predictions by taking  $D=0.25$  for mean value lifetime predictions into account. The relatively good coincidence in the 95%/95% case between the experimentally achieved data and the prediction curve based on the linear Palmgren-Miner rule may indicate, however, that the statistical failure probability is minimized by using 95% survivability prediction of lifetime, and that no further safety factors are needed. Looking to the effects of environment on fatigue, humidity had no significant influence in the area of commonly used maximum design strain levels (13).

It is clearly pointed out here that the results demonstrated can only be used for GFRP materials with mainly unidirectionally orientated fibres, and not yet for the life prediction of complex components like a spar beam of a wing or a rotor blade. Further basic knowledge of the fatigue behavior of other structural components must be gained first. Especially the fatigue properties of the shear web material must be investigated. Also other parameters like stress concentrations, manufacturing technology, and others may influence the lifetime. Thus, at the moment, further safety considerations cannot be omitted for the application of the described method to complete composite structures.

## 5. CONCLUSIONS AND OUTLOOK

A relatively simple but powerful lifetime prediction method for composite materials is presented and explained by three examples. It is based on s-n or  $\epsilon$ -n curves and the relevant constant amplitude life diagrams respectively, the linear Palmgren-Miner rule as well as the wind-energy specific load sequence WISPER/WISPERX. This standard was anticipated to be representative for other typical load spectra as well. The method will be validated in near future by an application also using the glider standard KoSMOS.

Considering the evaluation of the mean values, the comparison between experimental results and lifetime prediction yielded slightly conservative predictions for GI-Ep and the GI-UP2 combination, however, a non-conservative prediction for the other applied glass-polyester combination GI-UP1 with a damage factor of  $D=0.25$ , i.e. the experimental results showed here had a 4 times earlier failure than predicted. In the latter case, an additional safety margin must be introduced, for example, by the application of the relative Miner rule. If there is a lack of experimental data, the application of a damage sum  $D=0.1$  is proposed to compensate for uncertainty.

The evaluation of 95% survival probability and 95% lower confidence limit showed in all cases relatively good congruence between the experimentally defined and the life prediction curve. Thus the application of the 95%/95% curves for the described examples the lifetime prediction method yields satisfactory results, including the safety aspects.

Nevertheless the method described here will give more confidence when more experimental fatigue data are available. The lack of knowledge of the basic fatigue mechanisms requires caution and, thus, the application of relatively high safety factors for the lifetime for the general use of the method. In large structures, additionally the influence of stress concentrations, manufacturing methods and quality, and also complex stress conditions on the fatigue behavior should be considered. Taking those limitations into account, the fatigue lifetime prediction method

Material	Sequence	Damage accumulation sum D	
		Mean	95%/95%
Survivability			
GI-Ep	WISPERX	2.27	0.90
GI-UP1	WISPER	0.25	1.02
GI-UP2	WISPER	1.21	1.39

Table 4: Calculated damage accumulation sum D at a design strain level of 1% for GI-Ep, GI-UP1 and GI-UP2.

described here can be applied for non-constant load sequences.

## 6. REFERENCES

- (1) C.A. Patching, L.A. Wood, Further fatigue testing of a glass fiber reinforced plastic glider wing, *Technical Soaring*, Volume XXI, No. 1, paper read July 1997.
- (2) B.J. de Smet, P.W. Bach, DATABASE FACT, Fatigue of Composites for Wind Turbines, 3d IEA-Symposium on Wind Turbine Fatigue, 21-22 April 1994, ECN Petten, The Netherlands.
- (3) Ch. W. Kensche (ed.), Fatigue of materials and components for wind turbine rotor blades, European Commission, Directorate-General XII. Science, Research and Development (1996), ISBN 92-827-4361-6.
- (4) Ch. W. Kensche, Influence of composite fatigue properties on lifetime predictions of sailplanes, XXIV OSTIV Congress, Omarama, New Zealand (1995).
- (5) R. Mayer (ed.), Design of Composite Structures against Fatigue - Applications to Wind Turbine Blades, Mechanical Engineering Publications Ltd., Suffolk, UK (1996).
- (6) G.P. Sendeckyj, fitting Models to Composite Materials Fatigue Data, in: Test Methods and Design Allowables for Fibrous Composites, ASTM STP 734, C.C. Chamis, Ed. 1981, pp. 245-260.
- (7) J.C. Halpin, K.L. Jerina, T.A. Johnson, Analysis of Test Methods for High Modulus Fibers and Composites, ASTM STP 521, American Society for Testing and Materials, 1973, pp 5-64.
- (8) Richtlinie für die Zertifizierung von Windkraftanlagen, Chapter 5.2 Germanischer Lloyd, Ausgabe 1993.
- (9) L.J. Bain, Statistical Analysis of Reliability and Life-Testing Models, Theory and Methods, Marcel Dekker Inc., New York and Basel.
- (10) J.R. Soderquist, J.W. Bristow, Advanced Composites in Aircraft Structure, Seminar on Design/Certification Considerations in Composite Aircraft Structure, Basel, 24 to 26 April (1989).
- (11) A.A.v. ten Have, WISPER: A Standardized Fatigue Load Sequence for HAWT-blades, Proc. EEC, ed. W. Palz, Publ. Stephens & Ass., Bedford, England (1988).
- (12) Ch. W. Kensche, GFRP-Fatigue Data for Certification, Proceedings of the EWEC Conference and Exhibition, Thessaloniki, Macedonia, Greece, October 10-14 (1994).
- (13) Ch. W. Kensche, environmental Effects on GI-Ep Material and Tests on Blade Components with T-Bolt Load Attachment, DLR FB 94-09.